Letter

Failure of an effective stress approach in polydisperse wet granular materials

David Cantor[1,2,*] Emilien Azéma[3,4,†] and Carlos Ovalle[1,2,‡]

[1]*Department of Civil, Geological, and Mining Engineering, Polytechnique Montréal H3T 1J4, Canada*
[2]*Research Institute on Mining and Environment, RIME UQAT-Polytechnique, Montréal H3T 1J4, Canada*
[3]*LMGC, Université de Montpellier, CNRS, Montpellier 34090, France*
[4]*Institut Universitaire de France (IUF), Paris 75005, France*

(Received 17 June 2023; accepted 23 January 2024; published 8 April 2024)

In this Letter, the effective stress principle (ESP)—originally developed for granular materials saturated with water and recently extended to unsaturated ones via simulations—is shown to fail once the material presents wide grain size distributions. We demonstrate that the current ESP approaches cannot capture the Mohr-Coulomb strength parameters as soon as the grain size span exceeds $d_{\max}/d_{\min} \sim 4$. This failure is attributed to significant differences in the fabric generated by solid interactions in the wet material, which are supposedly capable of matching the characteristics of the dry material. We show that a generalization of the ESP requires not only macroscopic considerations but also direct attention to the nature of contact and force networks.

DOI: 10.1103/PhysRevResearch.6.L022008

Take a spoonful of any granular material—sand from a beach, soil from a garden, gravel next to a road. Those grains may display significant variation in sizes, shapes, and geological origins. The whole may also contain water or air within the pores, making it a complex mixture whose mechanical behavior is challenging to characterize.

While geotechnical engineering and physics of granular media have made significant progress over the last century, their theories still need meticulous scrutiny to prove themselves as cornerstones in these fields. Among these theories, the effective stress principle (ESP) stands out as a simple—yet robust—framework for addressing the mechanics of soils whose pores are filled with water (i.e., saturated soils). The ESP, attributed to Karl Terzaghi in the early 20th century [1,2], became common ground for studying soils. The principle states that the stresses on the solid phase of a granular material, coined *effective stresses* σ_{ij}^{eff}, control its shear strength and deformation, and can be estimated after subtracting the water pressure u_w from the total external stresses σ_{ij} (i.e., $\sigma_{ij}^{\text{eff}} = \sigma_{ij} - u_w\delta_{ij}$, with δ_{ij} the Kronecker delta operator).

The ESP proved highly successful, so it was natural to try extending it to unsaturated materials, where the pores are partially filled with water. These mixtures are also called wet materials when the water content is low. The first attempts to generalize the ESP are often attributed to Croney *et al.* [3], Aitchison [4], and Jennings [5], who proposed the relationship $\sigma_{ij}^{\text{eff}} = \sigma_{ij} - \chi u_w\delta_{ij}$, with u_w the water pressure derived from capillary bridges and χ an empirical parameter. Bishop *et al.* [6,7] extended this approach by including an air pressure u_a different than the atmospheric one, as $\sigma_{ij}^{\text{eff}} = (\sigma_{ij} - u_a\delta_{ij}) - \chi(u_a - u_w)\delta_{ij}$. However, these approaches were proven inaccurate as χ was identified as a parameter dependent on stresses and strains.

Alternatives were then developed based on two independent variables: the net stress $(\sigma_{ij} - u_a\delta_{ij})$ and matric suction $(u_a - u_w)$ [8]. Based on this strategy, extensive work on unsaturated material modeling was developed [9–11]. Yet, the search for an effective stress has never stopped and attempts to find a single stress variable are still reported [12–17]. To date, none is considered to be a complete generalization of the ESP.

More recently, works developed in the frame of the discrete-element method (DEM) have suggested that an effective stress approach could still be used for the description of shear strength in unsaturated materials [18–24]. Since DEM simulations can precisely define the liquid bridge forces between grain pairs, a capillary stress tensor σ_{ij}^{cap} can be directly computed, allowing for an extension of Terzaghi's ESP as $\sigma_{ij}^{\text{cont}} = \sigma_{ij} - \sigma_{ij}^{\text{cap}}$, with the solid contact stress $\sigma_{ij}^{\text{cont}}$ the candidate for the effective stress. This proposal has been received, however, with skepticism [20,25,26], since it only validates the ESP through numerical experiments. In addition, these works employed grain assemblies of similar sizes or with a relatively narrow size distribution. Experimental tests have also employed same-size particle assemblies [27]. It is important to note that these works focused on the shear strength properties. The elastic properties of these materials are still not captured by the solid contact stress definition $\sigma_{ij}^{\text{cont}}$ [22,28].

While several experimental and numerical works have shown that particle size distribution (PSD) does not affect the macroscopic shear strength in dry granular materials [19,29–38], understanding the effect of the PSD on wet granular materials has remained seldom explored. In particular, we

*david.cantor@polymtl.ca
†emilien.azema@umontpellier.fr
‡carlos.ovalle@polymtl.ca

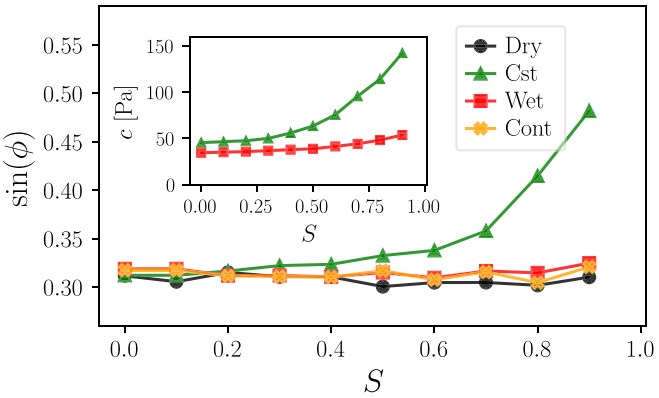

FIG. 1. Evolution of the macroscopic friction angle $\sin(\phi)$ and (inset) the cohesion c for the dry material (black circles), the constant force interaction law (green triangles), the wet law (red rectangles), and the solid contact stress tensor (orange crosses) as a function of particle size span S.

can summarize the questions that remain still unresolved in this topic as follows: (1) Is the macroscopic friction in wet granular materials independent of particle size polydispersity as it is in dry materials? (2) What are the effects of particle size polydispersity on macroscopic cohesion? (3) Is an effective stress approach still valid in wet size-dispersed granular materials? Advances in this field would not only benefit the soil mechanics community but also many other applications and industrial processes, such as particle mixing, segregation, flowability, and clustering [39–45].

In this work, we use a three-dimensional DEM approach called contact dynamics (CD) to investigate the shear strength of unsaturated granular materials interacting through pendular water bridges over a wide range of PSDs. The CD method is well suited to handle assemblies of rigid particles with diverse interaction laws, allowing body kinematics and contact forces to be resolved in a time-stepping scheme. For details about this method, please see Refs. [46–48]. We test the ESP as recently proposed in the literature and analyze whether or not it still holds once the dispersion of particle sizes is considered. Finally, a detailed micromechanical description of wet and dry samples allows us to unveil the elements that invalidate the current ESP approach after a certain grain size span. Note that this work does not attempt to propose a generalized version of the ESP notion, but rather aims to build a solid case to show that this theory needs to be reevaluated under the light of more realistic material conditions. More importantly, we show that a paradigm shift may be necessary to extend many of the observations and laws that have been developed for the mechanics of granular media.

The particle size span in a granular material can be characterized using the parameter $S = (d_{\max} - d_{\min})/(d_{\max} + d_{\min})$, where $d_{\max}$ and $d_{\min}$ are the maximal and minimal particle diameters in a sample. We built numerical samples using the free open-source simulation platform LMGC90 [49], varying S in the range $[0, 0.9]$, in steps of 0.1 (i.e., ten samples from monosize to highly polydisperse). The PSD followed a uniform distribution by volume fractions between $d_{\min}$ and $d_{\max}$ (see Fig. 1 in Supplemental Material [50]). The initial configuration of the samples is obtained after an isotropic compression of frictionless dry spheres that were placed in boxes using simple geometrical rules [51].

We considered two scenarios to simulate granular materials interacting with attractive capillary forces. First, we used a simple model with a constant attractive force f_0 acting between particles as long as they remain at a distance inferior to $\delta_{\max}$ to each other. The second model emulates water menisci as proposed by Soulié *et al.* [52] and Richefeu *et al.* [53] after experimental tests, where the capillary force f^{cap} and the distance $\delta_{\max}$ depend on the size of the particles and a volume of water at the capillary bridge. In this model, the force f^{cap} decays exponentially as the particles move apart. We set the water surface tension to 7×10^{-2} Jm^{-2} and the water content $w = m_w/m_s = 3\%$, with m_w and m_s the water and the solid masses, respectively, which reproduce pendular bridge conditions [53]. We considered a perfectly wetting liquid with a contact angle $\theta = 0^\circ$ [50] (the Supplemental Material contains detailed information about the contact laws). To differentiate the two laws, parameters computed for the first law carry the subscript "cst" for constant attractive force, while for the second law, "wet," is used for wet contact law.

To characterize the shear strength, we employ the Mohr-Coulomb failure criterion as $q = \mu p + C^\dagger$, with the deviatoric stress $q = (\sigma_1 - \sigma_3)$ and the mean pressure $p = (\sigma_1 + 2\sigma_3)/3$, considering triaxial conditions (i.e., $\sigma_2 = \sigma_3$). The stresses σ_1 and σ_3 are the major and minor principal stresses of tensor σ_{ij}, computed as $\sigma_{ij} = (1/V)\sum_{\forall c} f_i \ell_j$ [54,55], with V the volume of the sample, f the contact force vectors, and ℓ the branch vectors (i.e., vectors joining the center of particles in interaction). The macroscopic strength parameters (i.e., friction angle ϕ and cohesion c) are defined through the relations $\mu = 6\sin(\phi)/[3 - \sin(\phi)]$ and $C^\dagger = c\,6\cos(\phi)/[3 - \sin(\phi)]$.

We simulated triaxial tests under six different confinement pressures and a constant vertical velocity v on the top and bottom walls, reproducing quasistatic shearing. This was ensured by using the inertial number $I = \dot{\varepsilon} d\sqrt{\rho/\sigma_c} \ll 1$, with $\dot{\varepsilon} = v/z_0$ the rate of vertical deformation, z_0 the initial height of the sample, and ρ the grains' density [56,57]. We set I to 1×10^{-3}. The tests were performed up to a cumulative vertical deformation $\varepsilon = \Delta/z_0 = 0.6$, with Δ the added displacement of the upper and bottom walls. We also simulated samples with dry frictional interactions between grains. The friction coefficient was set to 0.4 between particles and zero between walls and particles. These friction coefficient conditions ensure that the principal directions of stresses align with the loading orientation, as done experimentally. Additionally, the response of the numerical simulations is comparable with many other works in the literature dealing with similar triaxial loading conditions. No gravity was used to avoid pressure gradients.

We found that the steady state was reached in all cases after $\varepsilon \sim 0.3$ (i.e., stable shear strength and sample volume under continuous deformation) and computed averaged values of stresses q and p in the range $\varepsilon \in [0.35, 0.5]$ (see the strength and solid fraction curves as a function of ε in Fig. 3 of the Supplemental Material [50]). We then computed the shear strength parameters after fitting these q and p values to the Mohr-Coulomb envelope.

We defined a characteristic capillary stress $\lambda = f^*/\langle d\rangle^2$, with f^* the average capillary force and $\langle d\rangle$ the average

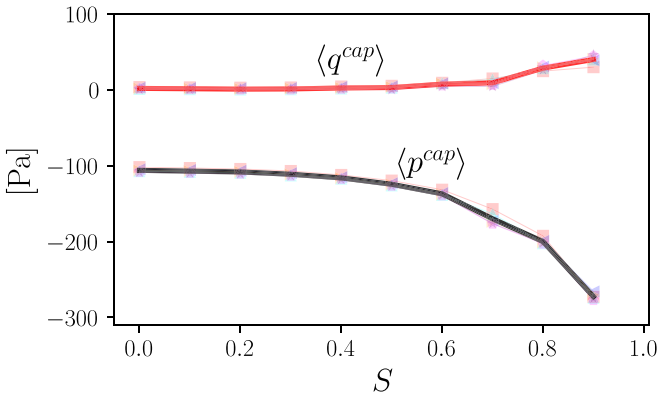

FIG. 2. Evolution of the capillary mean pressure p^{cap} and deviatoric stress q^{cap} as a function of S. Averaged values are shown since the different levels of η (shown in transparency) do not affect the tensor σ_{ij}^{cap}.

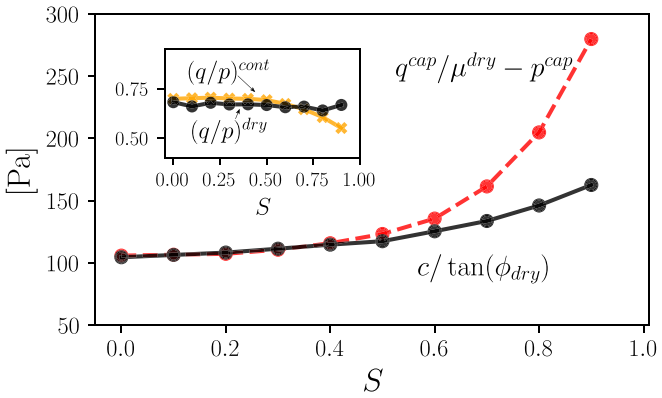

FIG. 3. Evolution of the macroscopic cohesion c and its prediction using the capillary stress tensor and the ESP as a function of the grain size span S. Inset: comparison between the ratio q/p for the dry material and "cont" network as a function of S.

particle diameter in each sample, and a dimensionless parameter $\eta = \lambda/p$, which provides a cohesion scale in each test. Clearly, $\eta = 0$ corresponds to the dry material, and as η increases either the capillary stress scale grows or lower confinement pressures are applied. Previous numerical tests have observed that values of $\eta > 2.5$ produce shear band formation [23], so to avoid those localization phenomena we considered values no larger than $\eta = 1.6$.

Figure 1 gathers the strength parameters as a function of the particle size span S for the two laws tested and the dry material. For the case with constant attractive force, both the macroscopic friction and cohesion increase with S, with increments in friction angle only remarkable after $S \sim 0.4$. For mono- or quasimonodisperse granular materials, the macroscopic friction $\sin(\phi_{\text{cst}})$ is indistinguishable from that in the dry material $\sin(\phi_{\text{dry}})$. However, macroscopic enhancements of shear strength with increasing particle polydispersity cannot only be attributed to increments in the macroscopic cohesion "c" as suggested in the literature [19]. Another implication of this behavior is that an effective stress approach cannot be applied as no connection between its shear strength and that of the dry material can be established. In turn, the wet material shows that only the macroscopic cohesion is affected by S. The macroscopic friction $\sin(\phi_{\text{wet}})$ is practically independent of the grain size span and remains fairly close to that of the dry material.

For the wet contact law, and following Refs. [18,23,58], the total stress tensor can be split into contributions by solid contact interactions and capillary bridges as $\sigma_{ij} = \sigma_{ij}^{\text{cont}} + \sigma_{ij}^{\text{cap}}$. Note that the total contact force between a particle pair is $f = f^{\text{cont}} + f^{\text{cap}}$. For interactions where the grains are separated a distance $\delta > 0$, f^{cont} is respectively zero.

The stress $\sigma_{ij}^{\text{cont}}$ is reminiscent of the effective stress because it represents the stresses in the solid phase after discounting the water contributions. However, σ_{ij}^{cap} is not necessarily a spherical tensor as shown in Refs. [59–61]—which debunks the early attempts to extend the ESP that considered a scalar (u_w) for the water contributions. Despite this difference, a macroscopic friction coefficient for solid contact interactions $\sin(\phi_{\text{cont}})$ can be identified by using the values of p^{cont} and q^{cont} from the tensor $\sigma_{ij}^{\text{cont}}$ (see Fig. 1). The values for $\sin(\phi_{\text{cont}})$ match the macroscopic friction angle of the dry material very well, suggesting that the solid contact stress σ^{cont} could indeed be a good candidate for the effective stress. Although this result is not new for mono- and quasimonosize grains, the fact that it still holds up for large grain size spans is shown here for the first time.

Regarding the capillary tensor σ_{ij}^{cap}, Fig. 2 displays the evolution of the mean pressure and deviatoric components, p^{cap} and q^{cap}, respectively, as a function of S. For grain size spans $S < 0.4$, the deviatoric component of σ_{ij}^{cap} remains relatively small and p^{cap} does not show remarkable variations. As larger particle size spans are considered, amplifications of mean pressure and deviatoric capillary stresses are observed, highlighting that σ_{ij}^{cap} has an anisotropic fabric that is accentuated with particle size polydispersity.

Based on the observations in Fig. 1, and imposing $q^{\text{cont}}/p^{\text{cont}} \equiv q^{\text{dry}}/p^{\text{dry}}$—i.e., considering $\sigma_{ij}^{\text{cont}}$ as the effective stress measure—it is possible to show that the macroscopic cohesion obeys the relationship

$$\frac{c}{\tan(\phi_{\text{dry}})} = \frac{q^{\text{cap}}}{\mu^{\text{dry}}} - p^{\text{cap}}, \tag{1}$$

with $\mu^{\text{dry}} = q^{\text{dry}}/p^{\text{dry}}$. The deduction of this equation appears in the Supplemental Material [50].

Figure 3 presents both sides of Eq. (1), i.e., the measured macroscopic cohesion and its estimation via the capillary stress tensor. The matching between these two curves is remarkable up to $S = 0.4$. Beyond this S, the right side of the equation progressively drifts away from the macroscopic measures. This mismatch no longer allows us to consider the stress partition in $\sigma_{ij}^{\text{cont}}$ and σ_{ij}^{cap} as a valid route for defining the effective stresses. In other words, our results show that the equivalency $\sigma_{ij}^{\text{cont}} \equiv \sigma_{ij}^{\text{dry}}$ is broken. When analyzing the components of these tensors, we detect a subtle but growing mismatch between the ratio q/p of the dry material and the "cont" network (see inset of Fig. 3). This discrepancy occurs despite the excellent agreement between the macroscopic friction angles $\sin(\phi_{\text{dry}})$ and $\sin(\phi_{\text{cont}})$ previously observed.

To understand the origins of this behavior, let us analyze the contact and force networks in the dry material, and the

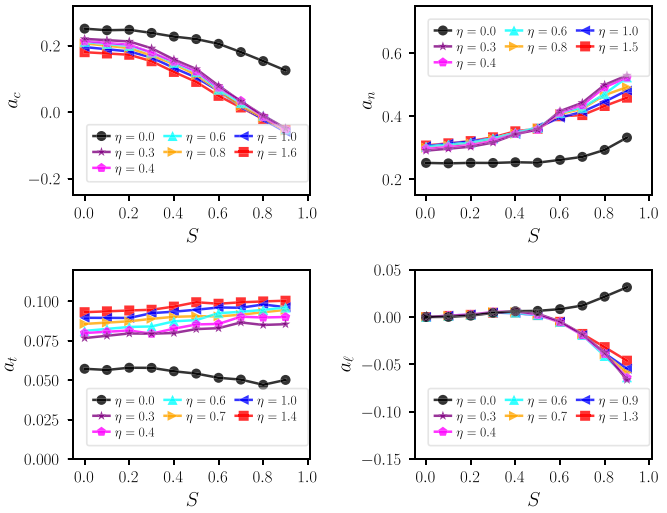

FIG. 4. Evolution of anisotropies linked to (a) contact orientations a_c, (b) normal forces a_n, (c) tangential forces a_t, and (d) branch lengths for the dry material (displayed with a black line) and the "cont" network for increasing level of cohesive scale η.

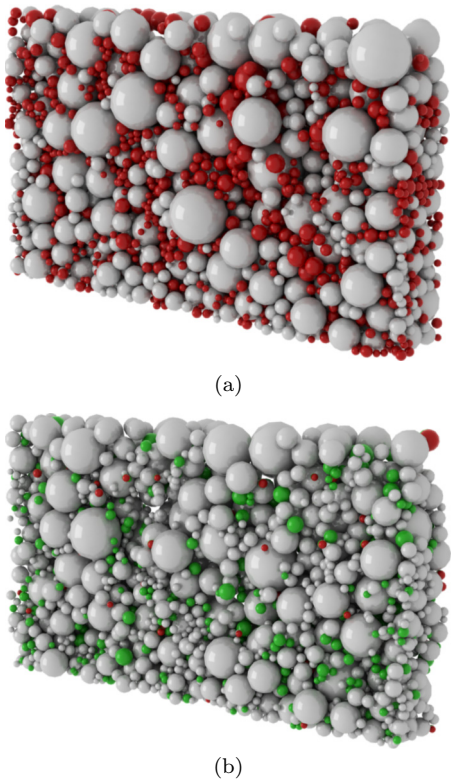

FIG. 5. Slices of the samples with particle size span $S = 0.8$ at level of deformation $\varepsilon = 0.3$, highlighting the grains carrying forces in gray and the floating particles in red for the (a) dry and (b) wet materials. For the latter case, grains that do not participate in the solid contact network are shown in green.

solid contact network in the wet material. Under triaxial conditions, the macroscopic strength can be estimated as $q/p \sim 2/5(a_c + a_n + a_t + a_\ell)$, where the right side of the equation is linked to anisotropies of contact orientations a_c, normal contact forces a_n, tangential contact forces a_t, and branch lengths a_ℓ. This expression is deduced after an analytical development of contact, force, and branch distributions in space and their mathematical description via spherical harmonics [62–64]. The validity of this approach has been well covered in the literature [19,34,65–68].

Figure 4 presents the evolution of these anisotropies, revealing that, even though the dry and "cont" components of the wet material exhibit equivalent macroscopic friction angles, this might be a fortunate coincidence. While for small particle size spans these anisotropies are relatively close to each other, the dry and solid contact fabrics are in reality different for all particle size spans. For instance, in a dry material it is acknowledged that the independence of shear strength on S is due to compensations between a drop of contact anisotropy a_c and increments of normal force anisotropy a_n (as S increases more contacts are found in all directions while the normal contact forces have a broader range and a more defined spatial orientation [19,31]). In the solid contact network, not only are there larger variations of a_c and a_n with S, but a_ℓ and a_t also evolve with different trends. The fact that a_c and a_ℓ decrease faster in the "cont" network suggests that (1) the grains within this network are better connected as S increases and (2) the preferential orientation of solid contacts differ from the dry case.

Dry granular materials are also known to contain an increasing amount of particles that do not contribute to the force transmission (i.e., floaters) as S increases. For instance, while the proportion of floaters P_0 is around 4% of the total number of grains in a monodisperse sample, it can reach more than 50% when $S = 0.9$ [34]. In contrast, P_0 never exceeds 0.5% in a wet material (see Fig. 5). It is thus unsurprising to find a better match between the macroscopic friction of the dry and wet materials for low values of S, as the number of floaters is relatively small in such cases. Further inspection of average stresses q^{cont} and p^{cont} also reveals that while for small S they are very well aligned, with q^{dry} and p^{dry} an increasing mismatching is noticeable beyond $S \sim 0.6$ (see inset in Fig. 3). This suggests that the mathematical construct behind $\sigma_{ij}^{\text{cont}}$—which is only supported by a simple contact force partition—is not fully capable of representing the effective stress in wet granular materials after a particle size equivalent to $d_{\max}/d_{\min} \sim 4$.

This series of analyses and observations allow us to conclude that (1) the macroscopic coefficient of friction remains independent of grain size polydispersity in wet granular materials where interactions between grains mimic capillary bridges; (2) size polydispersity enhances macroscopic cohesion; and, more importantly, (3) the current commonly accepted construction of the effective and capillary stress tensors for wet granular assemblies is no longer valid in a polydisperse granular material. While the decades-long quest to find an expression for effective stresses in unsaturated materials has yielded important insights into the mechanics of these materials, it has yet to fully succeed. Our observations show that this is due to the fact that current approaches do not consider different PSDs and the nature of granular networks that are assumed equivalent. At the same time, these differences open up avenues for repairing and generalizing the ESP. Future attempts need to focus on the role of the class of

floating particles in the dry material that are no longer rattling in the pore space of a wet material. It would also be interesting to revisit these results for different shapes of particle size distribution. Additionally, the preferential orientation of contact and force networks for solid contacts and capillary bridges are key elements to consider when evaluating the components of an effective stress network. However, it is important to acknowledge that these considerations quickly extend beyond the wet granular materials considered in this work. Recent and highlighted contributions in the fields of physics of granular media and soil mechanics which included attractive forces between grains (see, for instance, Refs. [69,70]) have dealt with materials with particle size spans below $d_{\max}/d_{\min} = 4$. Consequently, this study strongly suggests that those works should be reconsidered in the context of more realistic particle size distributions to confirm their universal character.

Further progress in this topic will also benefit from the development of three-phasic simulations (soil-water-air) that allow one to consider large grain size variability and the shape evolution of water bridges as the material is sheared. X-ray tomography and digital image correlations of grain-water mixtures [71] are also promising paths for improving our understanding on the mechanics of unsaturated granular materials.

This research benefited from the financial support of the Natural Sciences and Engineering Research Council of Canada (NSERC) (Project RGPIN-2019-06118) and the computational resources provided by Calcul Québec and Digital Research Alliance of Canada (Project RRG ID3604). We thank Mathieu Renouf and Fabien Soulié for their support in the development of the numerical simulations. We thank Franny McGill for copy-editing the manuscript.

[1] K. Terzaghi, *Erdbaumechanik auf bodenphysikalischer Grundlage* (Franz Deuticke, Leipzig, 1925).

[2] K. Terzaghi, *Theoretical Soil Mechanics* (Wiley, New York, 1943).

[3] D. Croney, J. D. Coleman, and W. P. M. Black, Movement and distribution of water in soil in relation to highway design and performance, Highway Research Board Special Report (1958).

[4] G. D. Aitchison, Relationships of moisture stress and effective stress functions in unsaturated soils, in *Proceedings Pore Pressure and Suction in Soils* (Butterworths, London, England, 1961), pp. 47–52.

[5] J. E. B. Jennings, A revised effective stress law for use in the prediction of the behavior of unsaturated soils, in *Proceedings of the Pore Pressure and Suction in Soils* (Butterworths, London, England, 1961), pp. 26–30.

[6] A. Bishop, I. Alpan, G. Blight, and I. Donald, Factors controlling the strength of partly saturated cohesive soils, in *Proceedings of the Research Conference on Shear Strength of Cohesive Soils* (ASCE, New York, 1960).

[7] A. W. Bishop and I. B. Donald, The experimental study of partly saturated soil in the triaxial apparatus, in *Proceedings of the 5th International Conference on Soil Mechanics* (Paris, France, 1961).

[8] D. G. Fredlund and N. R. Morgenstern, Stress state variables for unsaturated soils, J. Geotech. Eng. Div. **103**, 447 (1977).

[9] E. E. Alonso, A. Gens, and A. Josa, A constitutive model for partially saturated soils, Géotechnique **40**, 405 (1990).

[10] C. Jommi, Remarks on the constitutive modelling of unsaturated soils, in *Experimental Evidence and Theoretical Approaches in Unsaturated Soils* (CRC Press, Boca Raton, 2000), pp. 147–162.

[11] D. Sheng, D. G. Fredlund, and A. Gens, A new modelling approach for unsaturated soils using independent stress variables, Can. Geotech. J. **45**, 511 (2008).

[12] M. Nuth and L. Laloui, Effective stress concept in unsaturated soils: Clarification and validation of a unified framework, Int. J. Numer. Anal. Methods Geomech. **32**, 771 (2008).

[13] Y. Kohgo, M. Nakano, and T. Miyazaki, Theoretical aspects of constitutive modelling for unsaturated soils, Soils Found. **33**, 49 (1993).

[14] A. Modaressi and N. Abou-Bekr, A unified approach to model the behaviour of saturated and unsaturated soils, in *Proceedings of the 8th International Conference on Computer Methods and Advances in Geomechanics* (Balkema, Rotterdam, 1994), pp. 1507–1513.

[15] N. Khalili and M. H. Khabbaz, A unique relationship for χ for the determination of the shear strength of unsaturated soils, Géotechnique **48**, 681 (1998).

[16] N. Khalili, F. Geiser, and G. E. Blight, Effective stress in unsaturated soils: Review with new evidence, Int. J. Geomech. **4**, 115 (2004).

[17] E. E. Alonso, J.-M. Pereira, J. Vaunat, and S. Olivella, A microstructurally based effective stress for unsaturated soils, Géotechnique **60**, 913 (2010).

[18] P.-Y. Hicher and C. S. Chang, A microstructural elastoplastic model for unsaturated granular materials, Int. J. Solids Struct. **44**, 2304 (2007).

[19] C. Voivret, F. Radjai, J. Y. Delenne, and M. S. El Youssoufi, Multiscale force networks in highly polydisperse granular media, Phys. Rev. Lett. **102**, 178001 (2009).

[20] S. Khamseh, J.-N. Roux, and F. Chevoir, Flow of wet granular materials: A numerical study, Phys. Rev. E **92**, 022201 (2015).

[21] V. D. Than, S. Khamseh, A. M. Tang, J.-M. Pereira, F. Chevoir, and J.-N. Roux, Basic mechanical properties of wet granular materials: A DEM study, J. Eng. Mech. **143**, C4016001 (2017).

[22] J. Duriez, R. Wan, M. Pouragha, and F. Darve, Revisiting the existence of an effective stress for wet granular soils with micromechanics, Int. J. Numer. Anal. Methods Geomech. **42**, 959 (2018).

[23] M. Badetti, A. Fall, F. Chevoir, and J.-N. Roux, Shear strength of wet granular materials: Macroscopic cohesion and effective stress, Eur. Phys. J. E **41**, 68 (2018).

[24] J.-P. Wang, G.-H. Zeng, and H.-S. Yu, A DEM investigation of water-bridged granular materials at the critical state, Comp. Part. Mech. **6**, 637 (2019).

[25] B. Chareyre, Comment on "Flow of wet granular materials: A numerical study," Phys. Rev. E **96**, 016901 (2017).
[26] S. Khamseh, J.-N. Roux, and F. Chevoir, Reply to "Comment on 'Flow of wet granular materials: A numerical study,' " Phys. Rev. E **96**, 016902 (2017).
[27] M. Badetti, A. Fall, D. Hautemayou, F. Chevoir, P. Aimedieu, S. Rodts, and J.-N. Roux, Rheology and microstructure of unsaturated wet granular materials: Experiments and simulations, J. Rheol. **62**, 1175 (2018).
[28] C. Chalak, B. Chareyre, E. Nikooee, and F. Darve, Partially saturated media: From DEM simulation to thermodynamic interpretation, Eur. J. Environ. Civil Eng. **21**, 798 (2017).
[29] D. Muir Wood and K. Maeda, Changing grading of soil: Effect on critical states, Acta Geotechnica **3**, 3 (2008).
[30] G. Li, C. Ovalle, C. Dano, and P.-Y. Hicher, Influence of grain size distribution on critical state of granular materials, in *Constitutive Modeling of Geomaterials* (Springer, Berlin Heidelberg, 2013), pp. 207–210.
[31] D. H. Nguyen, E. Azéma, P. Sornay, and F. Radjai, Effects of shape and size polydispersity on strength properties of granular materials, Phys. Rev. E **91**, 032203 (2015).
[32] N. Estrada, Effects of grain size distribution on the packing fraction and shear strength of frictionless disk packings, Phys. Rev. E **94**, 062903 (2016).
[33] E. Azéma, S. Linero, N. Estrada, and A. Lizcano, Shear strength and microstructure of polydisperse packings: The effect of size span and shape of particle size distribution, Phys. Rev. E **96**, 022902 (2017).
[34] D. Cantor, E. Azéma, P. Sornay, and F. Radjai, Rheology and structure of polydisperse three-dimensional packings of spheres, Phys. Rev. E **98**, 052910 (2018).
[35] J. Yang and X. D. Luo, The critical state friction angle of granular materials: does it depend on grading? Acta Geotechnica **13**, 535 (2018).
[36] D. Cantor, E. Azéma, and I. Preechawuttipong, Microstructural analysis of sheared polydisperse polyhedral grains, Phys. Rev. E **101**, 062901 (2020).
[37] A. Gokce, Y. Yilmaz, Y. Deng, and C. S. Chang, Influence of particle size on the drained shear behavior of a dense fluvial sand, Acta Geotechnica **16** (2021).
[38] O. Polanía, M. Cabrera, M. Renouf, E. Azéma, and N. Estrada, Grain size distribution does not affect the residual shear strength of granular materials: An experimental proof, Phys. Rev. E **107**, L052901 (2023).
[39] A. Samadani and A. Kudrolli, Segregation transitions in wet granular matter, Phys. Rev. Lett. **85**, 5102 (2000).
[40] M. Scheel, D. Geromichalos, and S. Herminghaus, Wet granular matter under vertical agitation, J. Phys.: Condens. Matter **16**, S4213 (2004).
[41] A. Castellanos, The relationship between attractive interparticle forces and bulk behaviour in dry and uncharged fine powders, Adv. Phys. **54**, 263 (2005).
[42] A. Fingerle and S. Herminghaus, Unclustering transition in freely cooling wet granular matter, Phys. Rev. Lett. **97**, 078001 (2006).
[43] C.-C. Liao, S.-S. Hsiau, T.-H. Tsai, and C.-H. Tai, Segregation to mixing in wet granular matter under vibration, Chem. Eng. Sci. **65**, 1109 (2010).
[44] T. Trung Vo, S. Nezamabadi, P. Mutabaruka, J.-Y. Delenne, E. Izard, R. Pellenq, and F. Radjai, Agglomeration of wet particles in dense granular flows, Eur. Phys. J. E **42**, 127 (2019).
[45] Y. Ma, T. M. Evans, N. Philips, and N. Cunningham, Modeling the effect of moisture on the flowability of a granular material, Meccanica **54**, 667 (2019).
[46] F. Dubois, V. Acary, and M. Jean, The contact dynamics method: A nonsmooth story, C. R. - Mec. **346**, 247 (2018).
[47] F. Radjai and V. Richefeu, Contact dynamics as a nonsmooth discrete element method, Mech. Mater. **41**, 715 (2009).
[48] M. Jean, The non-smooth contact dynamics method, Comput. Methods Appl. Mech. Eng. **177**, 235 (1999).
[49] F. Dubois, M. Jean, M. Renouf, R. Mozul, A. Martin, and M. Bagnéris, LMGC90, in *10e colloque national en calcul des structures* (2011), p. 8.
[50] See Supplemental Material at http://link.aps.org/supplemental/10.1103/PhysRevResearch.6.L022008 for derivation of equations, a detailed description of the model material, and additional figures that provide support for the analysis of the material under critical state conditions.
[51] R. Jullien, A. Pavlovitch, and P. Meakin, Random packings of spheres built with sequential models, J. Phys. A: Math. Gen. **25**, 4103 (1992).
[52] F. Soulié, F. Cherblanc, M. El Youssoufi, and C. Saix, Influence of liquid bridges on the mechanical behaviour of polydisperse granular materials, Int. J. Numer. Anal. Meth. Geomech. **30**, 213 (2006).
[53] V. Richefeu, M. El Youssoufi, and F. Radjai, Shear strength properties of wet granular materials, Phys. Rev. E **73**, 051304 (2006).
[54] B. Andreotti, Y. Forterre, and O. Pouliquen, *Granular Media: Between Fluid and Solid* (Cambridge University Press, Cambridge, 2013).
[55] F. Nicot, N. Hadda, M. Guessasma, J. Fortin, and O. Millet, On the definition of the stress tensor in granular media, Int. J. Solids Struct. **50**, 2508 (2013).
[56] GDR-Midi, On dense granular flows, Eur. Phys. J. E **14**, 341 (2004).
[57] F. da Cruz, S. Emam, M. Prochnow, J.-N. Roux, and F. Chevoir, Rheophysics of dense granular materials: Discrete simulation of plane shear flows, Phys. Rev. E **72**, 021309 (2005).
[58] L. Scholtès, B. Chareyre, F. Nicot, and F. Darve, Micromechanics of granular materials with capillary effects, Int. J. Eng. Sci. **47**, 64 (2009).
[59] L. Scholtès, P.-Y. Hicher, F. Nicot, B. Chareyre, and F. Darve, On the capillary stress tensor in wet granular materials, Int. J. Numer. Anal. Methods Geomech. **33**, 1289 (2009).
[60] R. Wan, S. Khosravani, and M. Pouragha, Micromechanical analysis of force transport in wet granular soils, Vadose Zone J. **13**, 1 (2014).
[61] J. Duriez, M. Eghbalian, R. Wan, and F. Darve, The micromechanical nature of stresses in triphasic granular media with interfaces, J. Mech. Phys. Solids **99**, 495 (2017).
[62] L. Rothenburg and R. J. Bathurst, Analytical study of induced anisotropy in idealized granular material, Géotechnique **39**, 601 (1989).
[63] H. Ouadfel and L. Rothenburg, 'Stress-force-fabric' relationship for assemblies of ellipsoids, Mech. Mater. **33**, 201 (2001).
[64] X. Li and H.-S. Yu, Fabric, force and strength anisotropies in granular materials: a micromechanical insight, Acta Mech. **225**, 2345 (2014).

[65] E. Azéma, F. Radjai, and F. Dubois, Packings of irregular polyhedral particles: Strength, structure, and effects of angularity, Phys. Rev. E **87**, 062203 (2013).

[66] N. Guo and J. Zhao, The signature of shear-induced anisotropy in granular media, Comput. Geotech. **47**, 1 (2013).

[67] J. Zhao and N. Guo, Rotational resistance and shear-induced anisotropy in granular media, Acta Mechanica Solida Sinica **27**, 1 (2014).

[68] J.-P. Wang, X. Li, and H.-S. Yu, Stress-force-fabric relationship for unsaturated granular materials in pendular states, J. Eng. Mech. **143**, 04017068 (2017).

[69] T. T. Vo, S. Nezamabadi, P. Mutabaruka, J.-Y. Delenne, and F. Radjai, Additive rheology of complex granular flows, Nat. Commun. **11**, 1476 (2020).

[70] S. Mandal, M. Nicolas, and O. Pouliquen, Insights into the rheology of cohesive granular media, Proc. Natl. Acad. Sci. USA **117**, 8366 (2020).

[71] J. E. Andrade, Z. Gu, S. Monfared, K. A. M. Donald, and G. Ravichandran, Measuring Terzaghi's effective stress by decoding force transmission in fluid-saturated granular media, J. Mech. Phys. Solids **165**, 104912 (2022).